HL 38.15

Macroscopic dielectric function of perovskites by the ELAPW-kp method

contact: krasovsk@tp.cau.de
bahnsen@tp.cau.de
URL: www.tp.cau.de/schattke

E. E. Krasovskii, R. Bahnsen, O. V. Krasovska, and W. Schattke

Institut für Theoretische Physik und Astrophysik, Christian-Albrechts-Universität zu Kiel, Leibnizstraße 15, D-24098 Kiel, Germany

HIGHLIGHTS

⇒ **For the first time both the local field effects and the effects of spin-orbit coupling are included in the calculation of optical properties.**

⇒ **Studied are $ATiO_3$ cubic perovskites (A = La, Ba, Sr), in which the spin-orbit splitting of the atom A semicore *p* states is considerable. (see Fig. 1)**

⇒ **The intense dipole-allowed transitions from the *p* states to conduction band *d*-resonance states are strongly affected by the microscopic fields: the optical absorption band arising from these transitions occurs at an energy about several eV higher than the $p \to d$ excitation energy. (see Figs. 2 and 3)**

⇒ **Only for $LaTiO_3$ is observed a tangible effect of the spin-orbit interaction on the optical properties: it affects the fine structure of the far UV reflectivity band (around 20 eV). (see Fig. 4)**

⇒ **The optical properties of $LaTiO_3$ above ~2 eV are found insensitive to the details of the electronic structure Ti t_{2g} manifold. The agreement with the measurements is excellent, though a paramagnetic metallic band structure was adopted to calculate the optical properties of this Mott-Hubbard insulator. (see Figs. 2 and 4)**

⇒ **At low energies (up to ~15 eV) the spectra are formed by the charge transfer transitions from the oxygen 2*p* band to titanium 3*d* band. These excitations are found to be completely unaffected by the local fields. (see Fig. 5)**

Methodology

The macroscopic dielectric function (DF) $\varepsilon(\omega)$ is given by the matrix inverse of the dielectric matrix in the reciprocal space representation $\varepsilon_{\mathbf{GG}'}(\omega)$.[1] We start with constructing the dielectric matrix within the random phase approximation (RPA), for which a detailed knowledge of the band structure is required. In the long-wavelength limit the RPA expression for the microscopic dielectric matrix reads,[1]

$$\varepsilon_{\mathbf{GG}'} = \delta_{\mathbf{GG}'} - \frac{e^2}{4\pi^2 |\mathbf{G}||\mathbf{G}'|} \sum_{\lambda\lambda'} \int_{BZ} \frac{\langle \mathbf{k}\lambda' | e^{i\mathbf{G}'\mathbf{r}} | \mathbf{k}\lambda \rangle \langle \mathbf{k}\lambda | e^{-i\mathbf{G}\mathbf{r}} | \mathbf{k}\lambda' \rangle}{E_{\lambda'}(\mathbf{k}) - E_{\lambda}(\mathbf{k}) - \omega + i\eta} \, d\mathbf{k},$$

where **G** and **G**' are reciprocal lattice vectors, and $E_\lambda(\mathbf{k})$ and $|\mathbf{k}\lambda\rangle$ are band energies and eigenstates. The summation runs through occupied λ and unoccupied λ' states.

For $\mathbf{G} \neq 0$ the matrix elements $\langle \mathbf{k}\lambda' | \exp(i\mathbf{Gr}) | \mathbf{k}\lambda \rangle / |\mathbf{G}|$ are obtained straightforwardly from the PW expansion of the wave function. By the notation $\mathbf{G}=0$ the $\mathbf{q} \to 0$ limit of $\langle \mathbf{k}\lambda' | \exp(i\mathbf{qr}) | \mathbf{k}\lambda \rangle / |\mathbf{q}|$ is meant (the direction of the vector **q** is unimportant for cubic crystals). The limit is taken analytically, and the expression reduces to the matrix element of the momentum operator. (Computational details are explained in Ref. 2)

The effects of exchange and correlation are taken into account within the time dependent adiabatic LDA.

The band structure is calculated with the ELAPW-**kp** method,[3] which provides an accurate treatment of both the crystal potential[4] and the wave functions. Owing to the extension of the radial basis set the method yields reliable band structure in the energy region from –35 eV (Ti 3*p* states) to 40 eV above the Fermi level.

Density of states

Figure 1:
Red circles show the XPS spectrum of $LaTiO_3$ (Ref. 5). The UPS spectrum of Ref. 6 is shown by blue circles. (The curves are arbitrarily shifted in energy). The width of the upper valence band is well reproduced, but the semi-core bands according to the XPS data lie consistently deeper than the calculated ones.
For the semicore p states the spin-orbit splitting is 1 eV for Sr 4p, 1.9 eV for Ba 5*p*, and 2.1 eV for La 5*p* states.

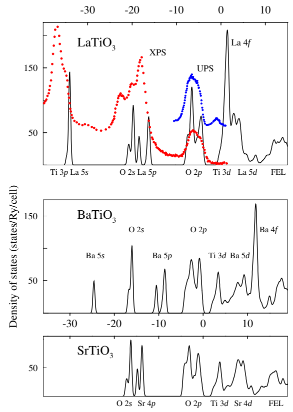

Discussion

In the IR part the experimental $LaTiO_3$ spectrum qualitatively differs from the spectra of the ''band'' semiconductors: the reflectivity grows with $\omega \to 0$ reflecting the narrow-gap nature of this Mott-Hubbard insulator. (To reproduce this behavior the Drude-like intraband contribution was artificially excluded from the dielectric function.)

In our ''metallic'' model the interband crystal-field transitions within the Ti t_{2g} manifold produce a steep increase of $\varepsilon_{00}(\omega)$ below 0.5 eV. In spite of a rather rough description of the occupied t_{2g} states, the present calculation yields a qualitatively correct picture of the IR reflectivity (Fig. 4).

The visible and near UV part of the spectra is determined by the charge transfer transitions from the oxygen *2p* band to titanium *3d* band, which is unoccupied in $BaTiO_3$ and $SrTiO_3$, but contains one electron in $LaTiO_3$ (see the density-of-states curve in Fig. 1). The transitions from the top of the O *2p* band to the top of the t_{2g} manifold give rise to the shoulder *A* at 5.75 eV in the optical conductivity spectrum $\sigma(\omega)$ (Fig. 2).

In the far UV range the reflectivity grows again due to the onset of transitions from the O 2*p* band to highly delocalized (free-electron-like, FEL) states above $E–E_F = 10$ eV. In the $\sigma(\omega)$ curve, Fig. 2, the O 2*p* → FEL excitations produce a broad band centered at $\hbar\omega = 20$ eV; its maximum is marked by the letter *D*. The O 2*p* → FEL contribution to $\sigma(\omega)$ overlaps with that from La 5*p* → 5*d* intra-atomic transitions (shaded area in Fig. 2).

For $SrTiO_3$ and $BaTiO_3$ the Sr 4*p* → 4*d* and Ba 5*p* → 5*d* contributions are shown in Fig. 3. The energy location of the intra-atomic peak changes strongly from perovskite to perovskite, whereas the O 2*p* → FEL band is very similar in the three substances. However, the pronounced intra-atomic structure does not survive the matrix inversion. A macroscopic $\sigma(\omega)$ function (solid lines in Figs. 2 and 3) cannot be separated into interband contributions, but superficially the effect appears as a redistribution of the $p \to d$ intensity over an energy interval to the right from the original peak.

Optical conductivity

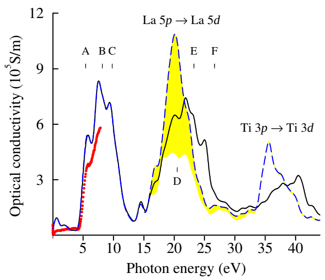

Figure 2:
Optical conductivity $\sigma(\omega) = \omega * \mathrm{Im}\, \varepsilon(\omega)/(4\pi)$ of $LaTiO_3$ with (solid line) and without local fields (dashed line). The yellow shaded area shows the contribution of the transitions from the semi-core La 5*p* states (predominantly La 5*p* → 5*d* excitations) to the optical conductivity spectrum calculated without local field corrections. Experimental data of Arima, Tokura, and Torrance[8], are shown by red circles.

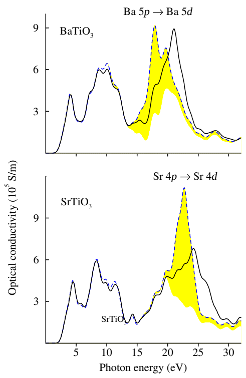

Figure 3:
Optical conductivity of $BaTiO_3$ and $SrTiO_3$ with (solid lines) and without local fields (dashed lines). The yellow shaded area shows the contribution of the transitions from the Ba 5*p* and Sr 4*p* states.

Reflectivity

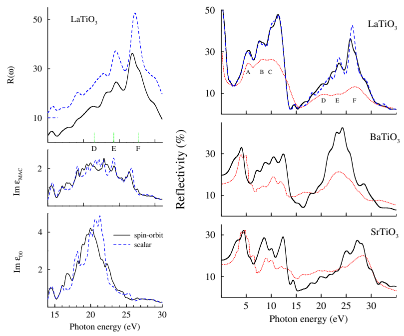

Figure 4:
left) The effect of spin-orbit coupling on the dielectric function and reflectivity of $LaTiO_3$. In the ε_{00} curve the main maximum is shifted to lower energies by ~1 eV due to an earlier onset of the transitions from the La $5p_{3/2}$ states. In the macroscopic function the effect is blurred out; still it remains important for the description of the fine structure of the reflectivity curve.

right) Reflectivity spectra of $LaTiO_3$, $BaTiO_3$, and $SrTiO_3$ perovskites derived from the macroscopic dielectric function (black lines). Red lines show the measurements by Arima and Tokura, Ref. 8, for $LaTiO_3$, and Cardona and Bäuerle *et al.* for $BaTiO_3$ and $SrTiO_3$, Ref. 9.

The effect of local fields

Figure 5:
Effect of local fields on the reflectivity (upper panel) and on the dielectric function (lower panel) of $LaTiO_3$. The nondiagonal matrix elements are seen to be negligible up to the onset of transitions from La 5*p* bands at ~18 eV. Dipole-allowed transitions from the localized La 5*p* and Ti 3*p* semi-core states generate strong local fields, which shift the peaks in the macroscopic DF curve to higher energies by several eV from the positions suggested by one-electron energy differences.

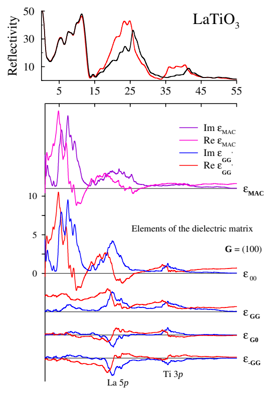

The La 5*p* → 5*d* absorption band shifts by 2 eV and broadens. The effect is caused by the Hartree contribution to the local fields. A detailed explanation has been presented in Ref. 2. The exchange-correlation contribution does not affect the shape of the spectra, but changes the absolute values: it tends to slightly reduce the effect.
Being not aware of such effects makes it often puzzling to compare the electronic band structure with optical spectra, as the main structures expected from pronounced density-of-states peaks are missing or shifted by several eV.

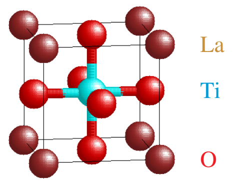

Figure 6:
$E2_1$ structure of ideal perovskites

[1] S . L. Adler, Phys. Rev. **126**, 413 (1962);
N. Wiser, Phys. Rev. **129**, 62 (1962).

[2] E. E. Krasovskii and W. Schattke, Phys. Rev. B **60**, 16251 (1999).

[3] E. E. Krasovskii and W. Schattke, Phys. Rev. B **56**, 12874 (1997).

[4] E. E. Krasovskii, F. Starrost, and W. Schattke, Phys. Rev. B **59**, 10504 (1999).

[5] D. J. Lam, B. W. Veal, and D. E. Ellis, Phys. Rev. B **22**, 5730 (1980).

[6] A. Fujimori, I. Hase, M. Nakamura, H. Namatame, Y. Fujishima,Y. Tokura, M. Abbate, F. M. F. de Groot, M. T. Czyzyk, J. C. Fuggle, O. Strebel, F. Lopez, M. Domke, and G. Kaindl, Phys. Rev. B **46**, 9841 (1992).

[7] T. Arima, Y. Tokura, and J. Torrance, Phys. Rev. B **48**, 17006 (1993).

[8] T. Arima and Y. Tokura, J. Phys. Soc. Jpn. **64**, 2488 (1995).

[9] M. Cardona, Phys. Rev. **140**, A651 (1965);
D. Bäuerle, W. Braun, V. Saile, G. Sprüssel, and E. E. Koch, Z. Phys. B **29**, 179 (1978).